scientific reports

Check for updates

OPEN

Simple and fast self-polymerization of benzidine using anodic exfloated graphene oxide nanosheet

Reza Dadashi[1], Khalil Farhadi[1,2]✉ & Morteza Bahram[1]

Nowadays, researchers are looking for green synthesis methods of polymers that solve the disadvantages of polymerization with different initiators and traditional methods. In this work, the self-polymerization process of benzidine by anodic exfloated graphene oxide Nanosheet electrode (AEGO Nsh) is reported for the first time in the world. The self-polymerization of benzidine onto AEGO Nsh electrode was done by an easy and simple method by anodizing the graphite sheet followed by immersing the AEGO Nsh electrode inside the benzidine monomer dissolved in organic and inorganic acid media. The surface morphology of the self-polymerized benzidine (SPB) onto the AEGO Nsh (SPB/AEGO Nsh) electrode was investigated by phone camera and scanning electron microscope (FE-SEM) imaging. The chemical characterization of the SPB/AEGO Nsh electrode was verified through XPS and ATR-IR analysis. Additionally, the self-polymerization of benzidine onto AEGO Nsh electrodes was confirmed by electrochemical tests using cyclic voltammetry (CV) and electrochemical impedance spectroscopy (EIS) techniques. The results from these investigations unequivocally confirm the self-polymerization of benzidine onto the AEGO Nsh electrode.

Keywords Self-polymerization, Polybenzidine, Anodizing, GO nanosheet, Green synthesis

Polymers are essential materials used in military, medical, engineering, transportation, and various industries[1]. Conductive polymers are a type of polymers that have wide applications in the manufacture of energy storage devices (batteries, supercapacitors), electronic equipment manufacturing industries, sensors, biosensors, medical equipment, etc[2,3]. The polymerization process of these polymers can be done in a traditional method and with the presence of initiators such as radical, anionic, cationic, etc. initiators[4–6]. Since the polymerization process with these expensive initiators is carried out in an acidic medium and in highly toxic organic solvents, which requires special and difficult conditions[7], researchers are looking for green synthesis methods to overcome these problems.

Self-polymerization is a method in which the polymerization process occurs spontaneously and is considered a green synthesis[7,8]. This method can be used as an alternative method for synthesizing polymers traditionally with different initiators due to reducing the cost and time of the polymerization process, saving energy, reducing environmental risks, and being safe[9,10]. Self-polymerization process can be done on different substrates or by using different catalysts. So far, researchers have polymerized a limited number of compounds with this method. Postma et al. have reported the single-step thin film assembly process on various SiO_2 particles via the oxidative self-polymerization of dopamine (DA) to form a range of single component polydopamine capsule systems[11]. Liu et al. have reported the self-polymerization of DA and polyethyleneimine (PEI-PDA) as fluorescent organic nanoparticles through self-polymerization of DA in the presence of PEI[12]. Chen et al. reported the self-polymerization of acrylic acid (AA) with methyl 3-(aziridin-1-yl) propanoate (MAP) at ambient temperature[13]. It is very important to use biodegradable and inexpensive substrates for the process of self-polymerization as a green and sustainable synthesis method for producing polymers. One of these substrates is graphite sheets, which can be performed the self-polymerization process on them by creating graphene oxide (GO) nanosheets, hydroxide, and radical groups through electrochemical processes[14,15].

Anodic exfoliation of graphite is a method that can increase the surface area of graphite sheets by creating a large number of graphene nanosheets. Anodic exfoliation method has many advantages over conventional exfoliation methods, including low-cost, simple operation, fast production-rate, and in-situ functionalization[16,17]. Electrochemical exfoliation process has been studied in various electrolytes which has been proven in particular, sulfate-containing electrolytes, such as H_2SO_4, $(NH_4)_2SO_4$ and K_2SO_4, showed exceptional exfoliation efficiency compared to other aqueous electrolyte systems[18]. in this method when potential is applied to the graphite

[1]Department of Analytical Chemistry, Faculty of Chemistry, Urmia University, Urmia, Iran. [2]Institute of Nanotechnology, Urmia University, Urmia, Iran. ✉email: khalil.farhadi@yahoo.com; kh.farhadi@urmia.ac.ir

electrode, anodic oxidation of water generates hydroxyl ions (OH^-) or oxygen radicals ($O^•$). The hydroxylation and oxidation reactions of these ions and radicals at the edges of graphite open up the edge sites, facilitating intercalation by anions, such as SO_4^{2-} [18] that these ions can act as initiators for self-polymerization reactions.

So far, the polymerization process of conductive polymers such as poly(p-aminophenol)[19], polyaniline, polythiophene, polypyrrole, poly(3,4-ethylenedioxythiophene) (PEDOT), etc. has been done by different initiators and in the traditional method and used in different fields[20–22]. Conductive polymers are used in various fields such as the removal of heavy metals and dye pollutants[23,24], electrochemical sensors[25,26], energy storage devices[27], etc.

Benzidine is a biphenyl aromatic diamine compound that has been polymerized with ammonium peroxydisulfate (APS) radical initiators. Polybenzidine (PB) and its composites have been used in fabricating energy storage devices[28], designing sensors[29] and developing different analytical methods[30,31]. To the best of our knowledge, there are no report about the self-polymerization of aromatic diamines especially benzidine in literature.

In this work, for the first time, the self-polymerization process of benzidine on anodized graphite sheet is reported. The use of this method and substrate is a starting point as a simple, cheap, and strong method for application in various industries and polymerization of other aromatic diamine compounds.

Materials and methods

Chemicals

Graphite sheet (99% purity and 0.5 mm thickness) was purchased from Alfa Aesar Company, K_2SO_4,

$NaHCO_3$, and benzidine ($\geq$ 99%) were purchased from Sigma-Alderich. All chemical reagents involving H_2SO_4, HCl, CH_3COOH, and $HClO_4$ were purchased from Merck and used without further purification. Double distilled water (DDW) was used to prepare all solutions.

Apparatus

DC power supply (DAZHENG, model PS-603D) was used for the anodizing process. The investigation of functional groups created on graphite sheets after the anodizing process and self-polymerization of benzidine was carried out by attenuated total reflection infrared (ATR- IR) spectra equipped with a Thermo Nicolet-USA spectrometer. Investigation of the surface morphology of the electrodes after anodizing, self-polymerization, and reduction of copper and nickel metals on GO nanosheets was done by a ZEISS Sigma VP scanning electron microscope (FE-SEM). X-ray photoelectron spectroscopy (XPS, ESCALAB 250Xi, Thermo Fisher) was employed to prove the formation of PB chain from self-polymerization onto anodic exfloated GO nanosheet (AEGO Nsh) electrode. Electrochemical studies to prove the stated claims were carried out by Autolab PGSTAT30 with a conventional three-electrode cell and electrochemical software (GPES version 4.9).

Creating GO nanosheets on graphite sheets (anodizing process)

First, graphite sheets (Gshs) were cut into 1 cm × 3 cm size and sonicated in water and ethanol for 10 min to clean their surface from any contaminations. All Gshs surfaces except the part to be anodized (1 cm×1 cm) were insulated using Teflon tape. The prepared Gshs were separately anodized in 0.1 M sulfuric acid, sodium bicarbonate, and potassium sulfate solutions. The anodizing process was carried out in a two-electrode system[32] in which a platinum sheet and a Gsh were selected as the cathode and anode, respectively. Two electrodes, anode and cathode, were placed parallel (distance 1 cm) to each other and were anodized in different solutions by applying a constant voltage of 10 V (0.5 A) for 150 s., then the other side of the Gsh was placed in front of the Pt electrode and anodized for 150 s. Finally, after finishing the anodizing process, the surface of the anodized graphite sheets (AEGO Nsh electrode) was washed several times with DDW and dried.

Self-polymerization process of benzidine

To carry out the self-polymerization process, first, a certain amount of benzidine monomer was prepared separately in different acid solutions. Then, AEGO Nsh electrode and the bare graphite sheet were immersed inside each of these solutions and after about 10 min, the AEGO Nsh and the bare graphite sheet electrode were taken out from the solution and washed with DDW and were dried in the oven at 50 °C for 5 h. Table 1 shows the different prepared solutions along with the benzidine monomer concentration.

Electropolymerization process of benzidine

The process of electrochemical polymerization of benzidine was carried out on a bare graphite sheet to investigate its electrochemical behavior with a PB that is self-polymerized using an AEGO Nsh electrode. According to previous studies[33], first, a solution containing 1 mM benzidine and 0.1 M acetic acid was prepared. Then, a graphite sheet electrode with a geometric surface area of 1 cm^2 was prepared, and finally, using the

Monomer concentration	Solution concentration	Solution
0.01 M	0.1 M	HCl
0.01 M	0.1 M	CH_3COOH
0.01 M	0.1 M	$HClO_4$

Table 1. Different prepared solutions along with benzidine monomer concentration for the self-polymerization process.

electrochemical method in a three-electrode system (the working, counter, and reference electrodes were bare graphite sheet, platinum sheet, and Ag/AgCl respectively) and with the CV technique. In the potential range of -1 to + 1 V, with a scan rate of 40 mV/s, it was polymerized for 10 cycles. Finally, the electrode was washed with DDW and dried to examine its electrochemical behavior.

Complying with relevant institutional, national and international guidelines and legislation. The authors declare that all relevant institutional, national, and international guidelines and legislation were respected.

Results and discussion

Morphological studies of the self-polymerization of PB onto AEGO Nsh electrode

The appearance properties and morphological of each of the substrates were studied at each stage by phone camera (Samsung Galaxy A31) and scanning electron microscope (FE-SEM) imaging, respectively. After immersing the electrodes inside each of the different acidic solutions containing benzidine monomer, the electrodes were taken out of the solution and their surface was photographed by phone, this process was checked during, before, and after the self-polymerization process. Figure 1a and b show images of bare graphite electrodes, AEGO Nsh electrode anodized in K_2SO_4 solution, and self-polymerized benzidine onto AEGO Nsh electrode (SPB/AEGO Nsh), after and during the self-polymerization process in acetic acid solution. As it is clear in this figure and video1 (https://drive.google.com/file/d/1oxeyJIPz7kuJviPcMnKJ-GBsmRBkFN9k/view?usp=sharing), after immersing the AEGO Nsh electrode inside the solution containing benzidine monomers, the polymerization process starts, and a layer of PB polymer is formed spontaneously on the surface, which is completely visible to the unaided eye, and it is a preliminary confirmation of the claim of self-polymerization of this monomer on the AEGO Nsh electrode.

To investigate the effect of the type of anodizing solution on the self-polymerization process, the graphite sheet electrode was also anodized in sulfuric acid and sodium bicarbonate solutions, and like the previous electrode to check the self-polymerization of benzidine onto these electrodes, the AEGO Nsh electrodes were immersed in the acetic acid solution containing benzidine monomer. Figure 2a and b show the pictures of the anodized electrodes in H_2SO_4, $NaHCO_3$ solutions and the polymerization process of benzidine on them, respectively. As it is clear in the pictures, after immersing the electrodes in the benzidine monomer solution, the polymerization process takes place and it shows that the polymerization process of benzidine can be formed on the anodized electrodes in other electrolytes. This can be attributed to the formation of hydroxide radicals and trapped electrons during the anodization process on the GO nanosheets created on the surface of the graphite sheets.

Morphological studies of the surface of different electrodes were further investigated by FESEM analysis. Figure 3 shows the FESEM images of bare graphite electrodes, AEGO Nsh electrodes anodized in K_2SO_4 solution, and self-polymerization of benzidine in CH_3COOH, HCl, and $HClO_4$ on the AEGO Nsh electrode. According to the FESEM images, the bare graphite sheet electrode has a smooth and almost uniform surface (Fig. 3a), after the anodizing process, due to the formation of GO nanosheets on its surface, the morphology of its surface changes a rough and non-uniform state (Fig. 3b). Figure 3c shows the FESEM image of the SPB/AEGO Nsh electrode in which the self-polymerization of benzidine occurred in the CH_3COOH solution. As it is clear in this image, PB is self-polymerized in the form of crystalline structures and specific morphology on the surface of this electrode. Figure 3d and e show the FESEM images of the SPB/AEGO Nsh electrode that the benzidine self-polymerization process took place on the electrode in HCl and $HClO_4$ solutions. As it is clear from these images, the morphology and amount of self-polymerization in the HCl, and $HClO_4$ solution (mineral acids environment) is different from the CH_3COOH solution (organic acid environment). The reason for this result is probably due to some characteristics of acetic acid, including providing a suitable environment for

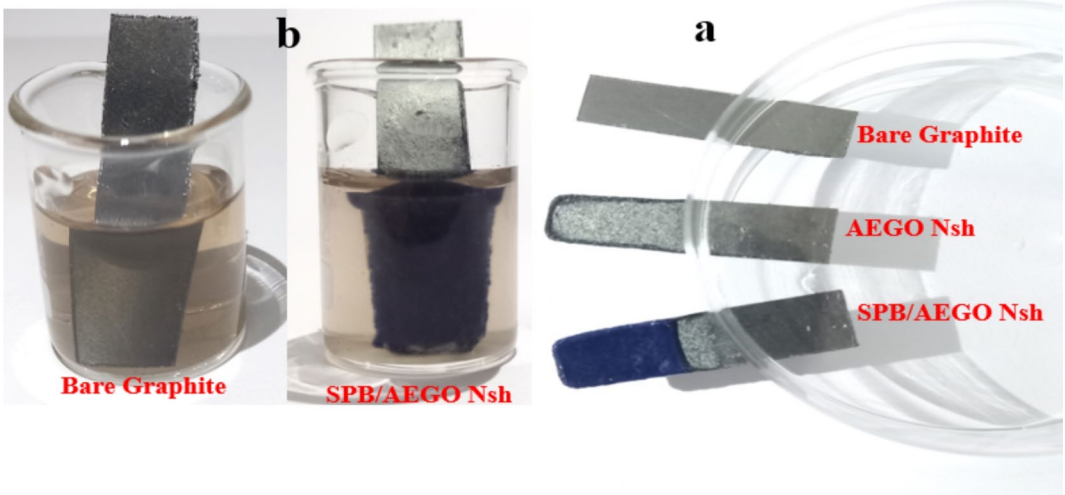

Fig. 1. The appearance image of different electrodes after (**a**) and during immerse (**b**) inside acetic acid solution containing benzidine monomer.

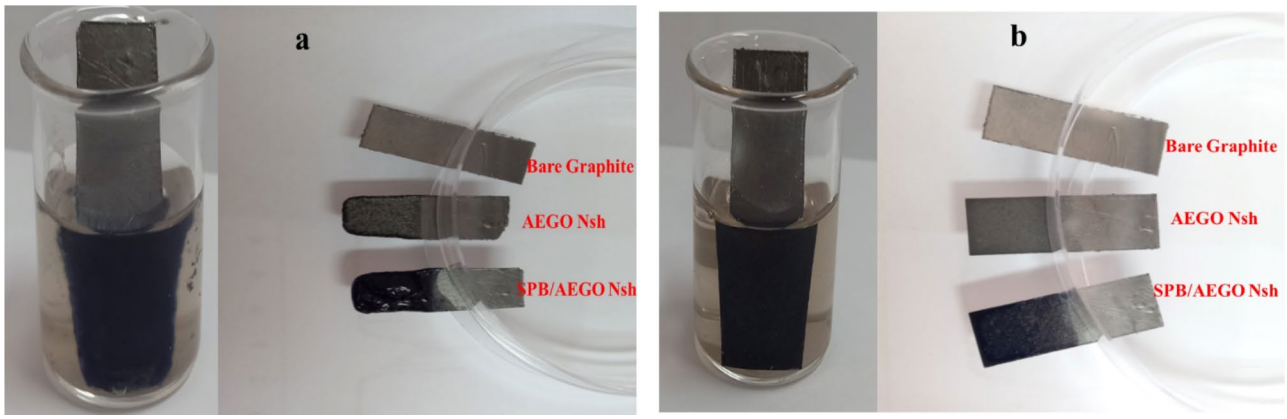

Fig. 2. The appearance image of different anodized electrodes in H_2SO_4 (**a**) and $NaHCO_3$ solution (**b**) during and after immerse in acetic acid solution containing benzidine monomer.

self-polymerization reaction, affecting the rate and efficiency of polymer formation. In this reaction, acetic acid may act as a mild acid catalyst and promote the reaction between monomers by facilitating proton transfer. This feature can increase the reactivity of functional groups and lead to more efficient polymer formation. Also, the buffering properties of acetic acid can help maintain optimal pH during the polymerization process. Another important factor may be related to the stabilization of reactive intermediates or radicals formed during the self-polymerization process by acetic acid, which helps to control the reaction pathway and improve the yield. Figure 3f shows SEM images of a cross-section of the SPB/AEGO Nsh electrode. As it is clear in this figure, the thickness of SPB formed on the AEGO Nsh electrode is about 19.44 µm.

Determining the possible mechanisms of the self-polymerization process of benzidine on AEGO Nsh electrode

The self-polymerization process of benzidine onto AEGO Nsh electrode can occur by the hydroxyl radical and trapped electrons among the GO nanosheets created during the electrochemical anodization process. As mentioned in the previous section, electrochemical anodizing was done in different solutions by applying a constant potential of 10 V (0.5 A). In this process, by applying voltage, the water splitting process occurs and hydroxyl radicals are produced, which are accumulated among the graphite layers by forming a weak bond[34,35]. The following reactions (Eqs. 1,2) show the water-splitting process during electrochemical anodization and the products produced[33,34].

$$H_2O \xrightarrow{e^-} {}^{-}OH + H^+ \tag{1}$$

$$H_2O \xrightarrow{e^-} {}^{\cdot}OH + H^+ \xrightarrow{e^-} {}^{\cdot}O + H^+ \tag{2}$$

In the next step, the available hydroxyl ions between the graphite layers react with the graphene oxides created on the graphite surface and form hydroxyl groups on the graphene surface (Eq. 3)[36,37]. At this stage, all the radicals produced are not converted into hydroxyl groups on the surface of graphene, and therefore some of them remain free among the graphite layers.

$$2C\,(\text{in graphene}) + 2\,H_2O \rightarrow 2C - OH(\text{in graphene}) + 2H^+ + 2e^- \tag{3}$$

The basis for the formation of hydroxyl groups on GO sheets is probably due to the attack of nucleophilic $^{\cdot}OH$ and $^{\cdot}O$ ions on the C sp^2 at the edges or defects in the graphite network. As it is clear in Eq. 3, during the conversion of $^{\cdot}OH$ into hydroxyl groups, some free electrons are also released due to the oxidation process, and with the progress of the reaction, a few hydroxyl groups on graphene oxides are oxidized to epoxy and carbonyl groups, and with the continuation of this process, some of the C-O groups on the surface are oxidized to CO and CO_2 according to reactions 4 and 5 (Eqs. 4,5):[37–39].

$$C + H_2O \rightarrow CO + 2H^+ + 2e^- \tag{4}$$

$$C + 2H_2O \rightarrow CO_2 + 4H^+ + 4e^- \tag{5}$$

In addition to the oxidation of ^{-}OH, the created O^{2-} ions can also react with carbon in graphene and create carbon O_2, CO_2, CO and free electrons (Eq. 6).

$$2H_2O \xrightarrow{e^-} 2O^{2-} + 4H^+ \rightarrow O_2 + 4H^+ + 4e^- \tag{6}$$

According to the reactions that occurred during the electrochemical anodization process, some produced $^{\cdot}OH$ ions in this process and the electrons released with the progress of each step of the reaction are trapped between

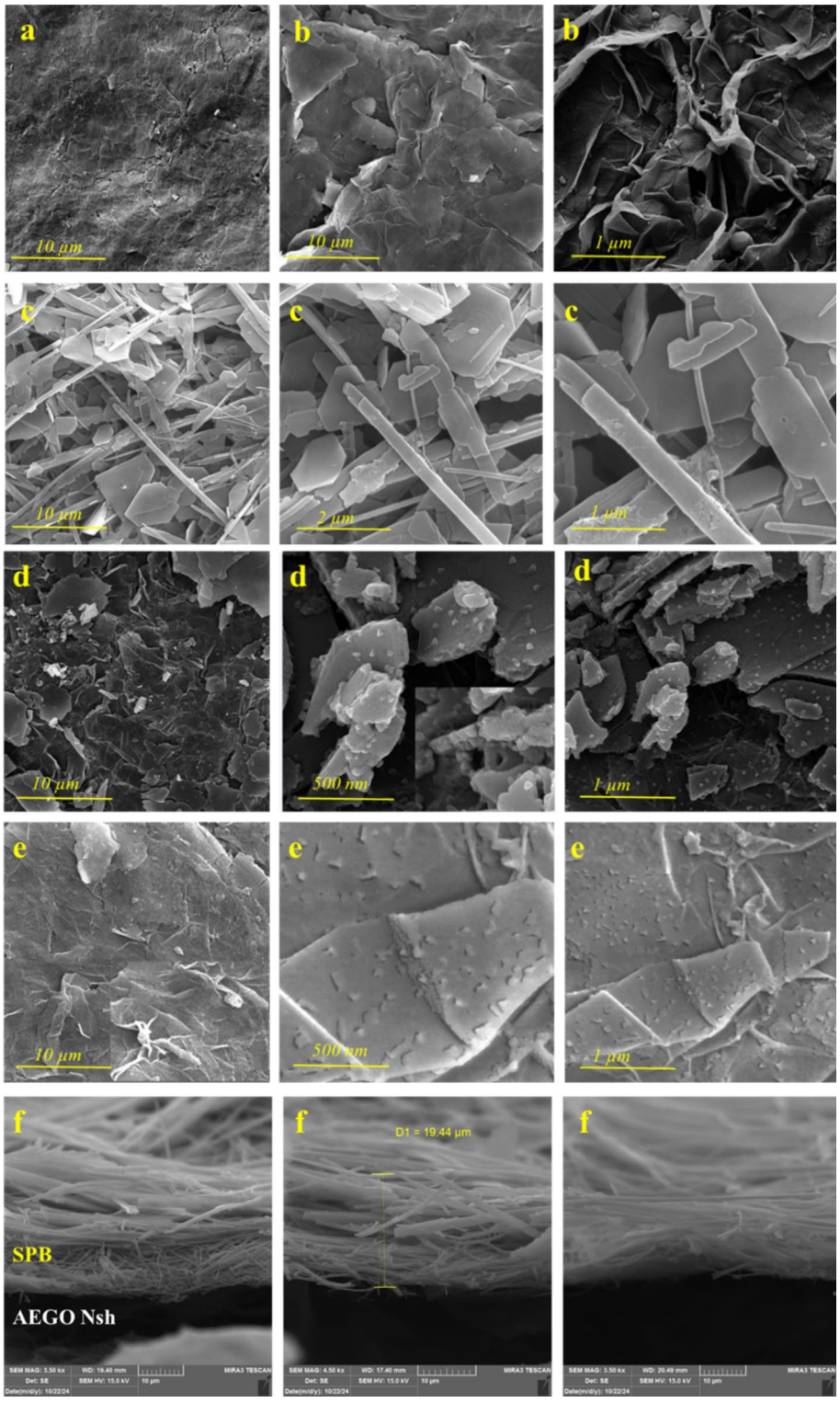

Fig. 3. FE-SEM images of bare graphite electrode (**a**), AEGO Nsh electrodes anodized in K_2SO_4 solution (**b**), self-polymerization of benzidine in CH_3COOH (**c**), HCl (**d**), and $HClO_4$ (**e**) on the AEGO Nsh electrode, and FE-SEM images of the cross-section of the SPB/AEGO Nsh electrode (**f**).

the graphite layers and the created GO nanosheets, which are strong possibility can act as an initiator to start the self-polymerization reaction of benzidine on the AEGO Nsh electrode.

Considering that benzidine is an aromatic diamine compound and can act as an electron donor from two sides in para positions, therefore, each monomer can attack from one para position to another para position of the monomer, and thus the self-polymerization process begins. This process probably happens in the presence

of •OH ions and trapped electrons between the layers of GO and graphite during the anodization process. The mechanism of polymerization as initiation, propagation and termination processes in the presence of •OH ions and trapped electron inside the layers of GO and graphite are reported in Figs. 4 and 5.

Physicochemical characteristics of the SPB onto AEGO Nsh electrode

The physicochemical characteristics of the SPB/AEGO Nsh electrode were carried out by X-ray photoelectron spectroscopy (XPS) and Attenuated Total Reflectance (ATR-IR) analyses to further prove the self-polymerization process.

Figure 6 shows the chemical characteristics recorded for the SPB/AEGO Nsh electrode by the XPS analysis. The appearance of the peaks related to elements N 1s, O 1s, and C 1s strongly confirms the self-polymerization process (formation of benzidine polymer chains) of benzidine onto AEGO Nsh electrode.

Figure 6a depicts the survey spectra of the SPB/AEGO Nsh electrode. Figure 6b and c, and d show the core-level spectra of N 1s, O 1s, and C 1s, respectively. In Fig. 6b, two Gaussian peaks with binding energy of 398.3 and 399.6 eV are related to imine-like structure (-N=) and unmodified amine-like nitrogen atoms (-NH) of PB chain[40–42]. The peaks related to C=O, C-OH, and C-O groups in the PB structure on the AEGO Nsh graphite electrode with binding energies of 530, 531.2, and 529 eV are shown in Fig. 6c[43,44], Also, these peaks can probably be attributed to the C=O, C-OH and C-O groups that were created as a result of the anodizing process on the graphite sheet[36]. Figure 6d depicts the C1s XPS core level spectra of the SPB/AEGO Nsh electrode. The major peak line can be decomposed into four peak lines: 282.2 eV (C=C), 283.1 eV (C–C sp^2), 284 eV (C–N) and 285 eV (C=O/C–O).[45]. The C–O/C=O functional groups present in the electrode is assigned to the formation of BQ (p-enzoquinone) in PB chains onto AEGO Nsh electrode[46,47]. Finally, according to Fig. 6e, two Gaussian peaks with binding energy of 166.5 and 167.75 eV are related to S–O and S=O of SO_2 which is produced in the anodizing process of the graphite sheet inside the K_2SO_4 solution due to the conversion of sulfate ions to SO_2[18,48,49] that can be trapped between the Go nanosheets layers.

Functional groups that appeared for PB structure in the XPS profile were also confirmed by ATR-IR spectroscopy. Figure 7 shows the ATR-IR spectrum of bare graphite, AEGO Nsh, and SPB/AEGONsh graphite electrodes. As seen in the ATR-IR spectrum of AEGO Nsh electrode, the peak related to the O-H group, which is caused by the anodization process of the middle and edges of the GO Nsh electrode and graphite, appeared at the wavelength of 1700 cm^{-1}.[50] Also, the peaks appearing at the 1070 and 1428 cm^{-1} are related to the C-O and C=O functional groups, respectively, due to the oxidized a few hydroxyl groups on graphene oxides to epoxy and carbonyl groups[36,50]. The appearance of these peaks in the ATR-IR spectrum and XPS profile, certainly confirms the possible mechanisms proposed for the proposed self-polymerization process. The peaks that have appeared in the ATR-IR spectrum of the SPB/AEGO Nsh electrode, confirm the formation of PB chains on the EGO Nsh electrode. According to the ATR-IR spectrum of the SPB/AEGO Nsh electrode, the peak appearing

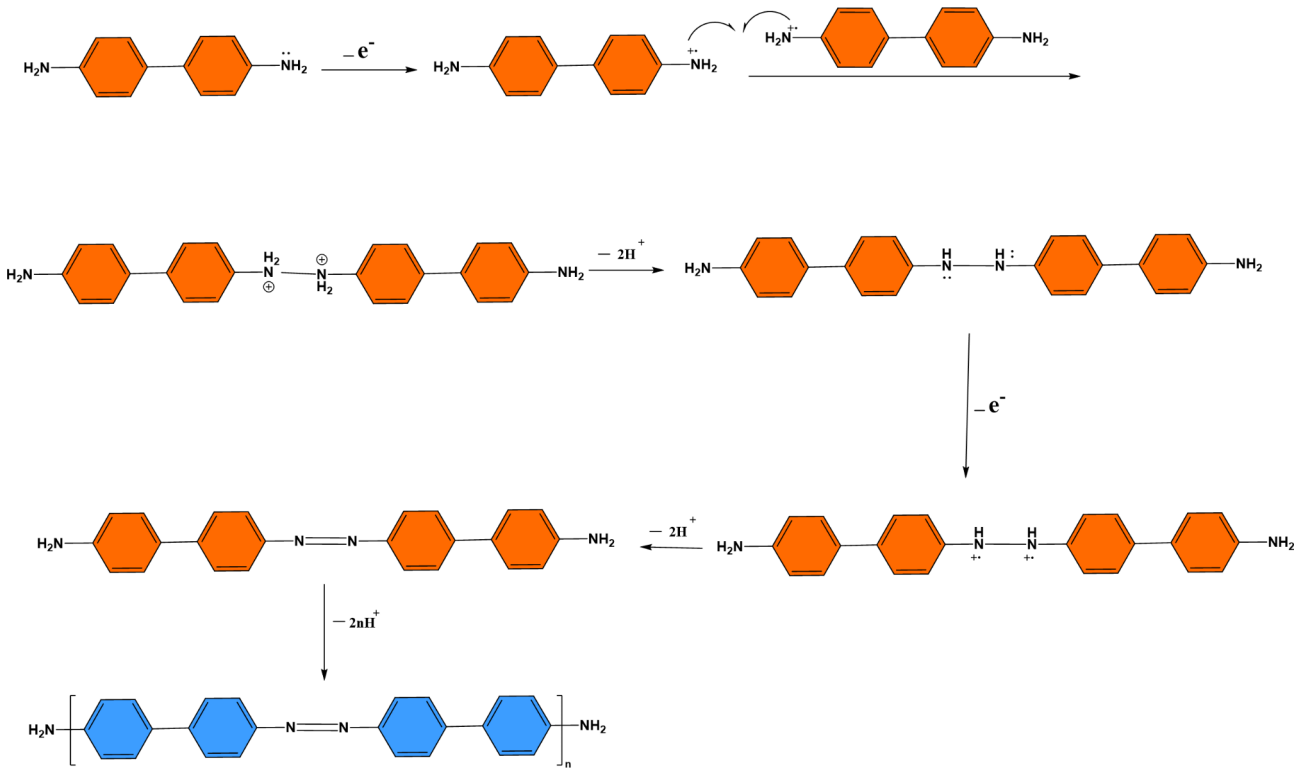

Fig. 4. The mechanism of the self-polymerization reaction of benzidine onto AEGO Nsh electrode by trapped electrons inside the GO and graphite layers.

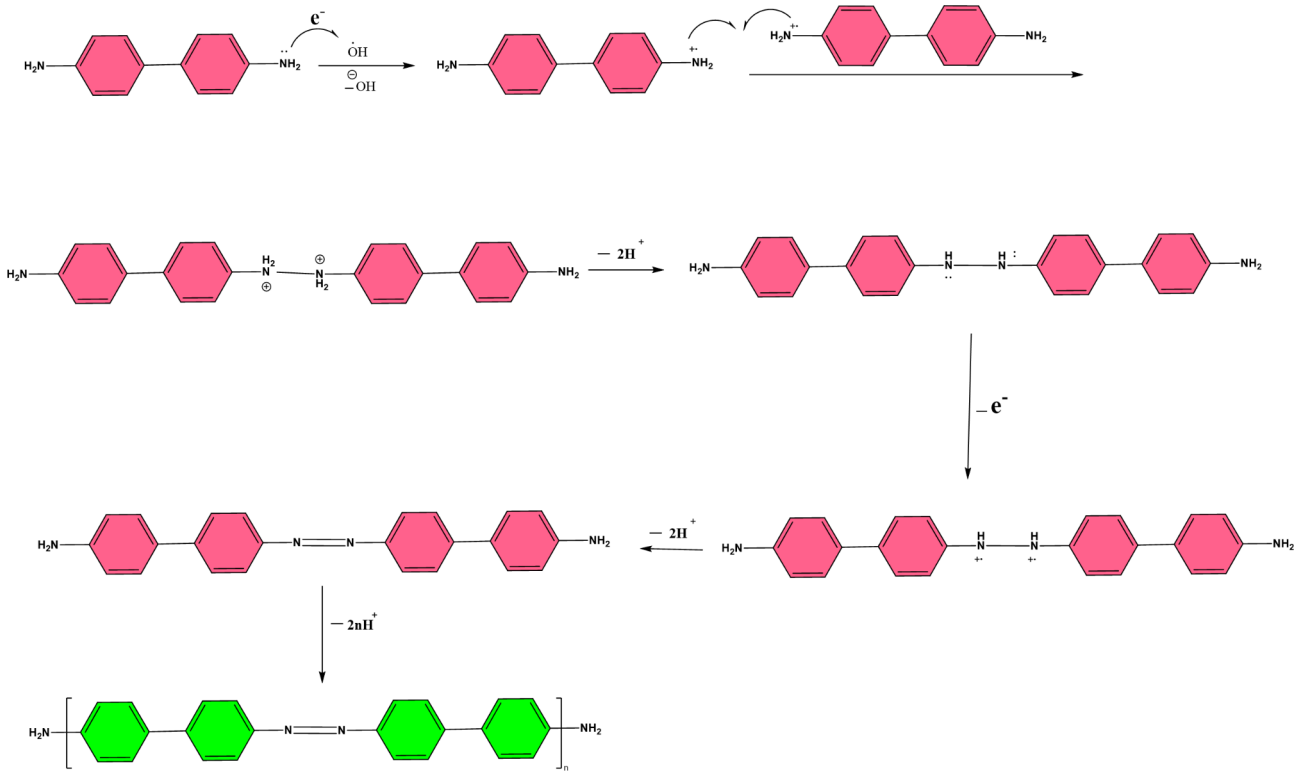

Fig. 5. The mechanism of the self-polymerization reaction of benzidine onto AEGO Nsh electrode by •OH ions inside the GO and graphite layers.

at of 3436 cm^{-1} corresponds to the stretching vibration bands of N-H[51,52]. The absorption peak of 2925 cm^{-1} is related to the stretching vibrations of the C-H group[53]. As it is clear in this spectrum, the peak related to the hydroxyl group created by the anodizing process at 1700 cm^{-1} has been removed due to participation in the self-polymerization reaction, and absorption bands have appeared at 1610, 1502, and 1305 cm^{-1}, which are related to the bending vibrations of the NH_2, C=C and C-N stretching vibrations of the quinoid ring in the structure of the PB chain, respectively[28,51,52]. The peak at 803 cm^{-1} was characteristic of the out-of-plane N-H bending vibration[28]. Finally, checking the chemical characteristics of the SPB/AEGO Nsh electrode by ATR-IR and XPS analyses like the morphological characterization proved the spontaneous formation of PB chains.

Electrochemical characteristics of the SPB onto AEGO Nsh electrode

After proving the self-polymerization process by physical and chemical characteristics, electrochemical techniques were used for further investigation. In this study, cyclic voltammetry (CV) and electrochemical impedance spectroscopy (EIS) techniques were used to investigate the electrochemical behavior of different electrodes. Electrochemical investigations were carried out in a three-electrode system in 1 M H_2SO_4 solution. In this configuration, Ag/AgCl electrode and platinum sheet were used as reference and auxiliary electrodes, respectively, and various synthesized electrodes with a surface area of 1 cm^2 were used as working electrodes. CV technique is one of the most ordinary electrochemical methods that can provide information about the kinetics of electrode reactions, homogeneous and heterogeneous electron transfers, as well as coupled reactions[54]. One of the most important applications of the CV technique is the study of control steps and electrochemical reaction mechanisms. In this study, the CV technique was used to study the redox reaction mechanism of PB. Figure 8a shows the CV curves of bare graphite electrode and AEGO Nsh electrodes that are anodized in different solutions of K_2SO_4, H_2SO_4, and $NaHCO_3$ at 30 mv s^{-1} in 1 M H_2SO_4 at 25 °C. As it is clear in this curve, the highest Faradaic current (capacitance) obtained for the anodized electrode in K_2SO_4 solution, which is probably due to the high ability of this electrolyte in the same conditions and in the presence of high voltages (10 V). As it has already been proven, the anodizing process of graphite sheet in SO_4^{2-} solutions shows higher efficiency and better performance in the production of GO[18,55,56]. The high ability of K_2SO_4 electrolyte in the anodizing process and creating GO nanosheets is probably due to the penetration of potassium ions between graphite layers and the expansion of the distance between the layers in order to easily exfoliate graphite into GO sheets. On the other hand, the use of K_2SO_4 solution provides a controlled ionic environment that can help maintain consistent conditions during the anodizing process. This control can lead to more uniform exfoliation and higher yields[55]. Overall, the combination of these factors make potassium sulfate as an effective electrolyte in the anodizing process to produce high yield graphene oxide from graphite sheets. These results were confirmed by the CV technique.

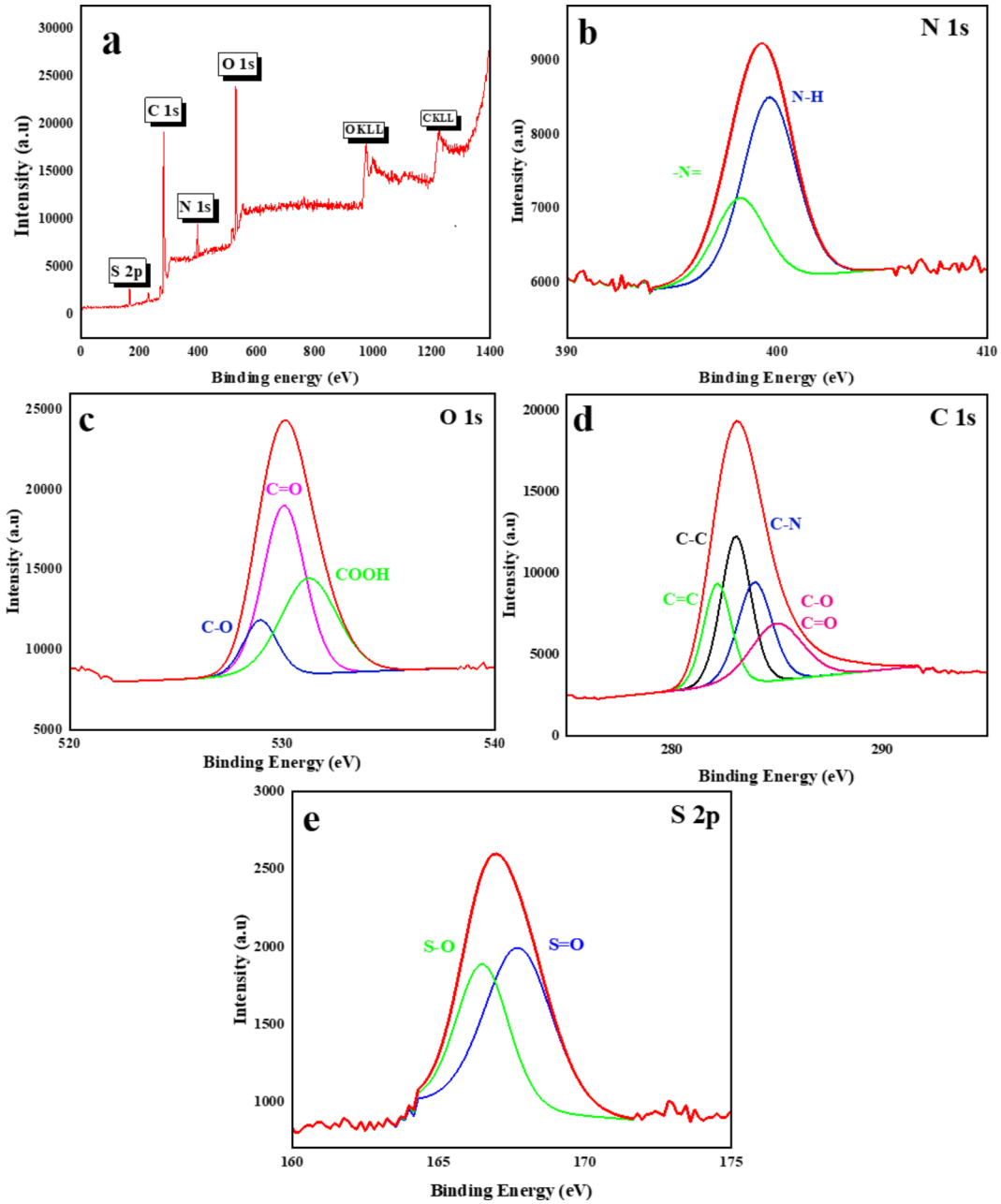

Fig. 6. XPS wide scan spectra of the SPB/AEGO Nsh electrode: (**a**) survey spectrum, (**b**) N1s spectrum, (**c**) O1s spectrum, (**d**) C1s spectrum, and (**f**) S2p spectrum of SPB/AEGO Nsh electrode.

Figure 8b shows the CV curves of SPB/AEGO Nsh electrodes (resulting from the self-polymerization of benzidine in CH_3COOH in the presence of prepared AEGO Nsh electrodes in different solutions) in 1 M H_2SO_4 after 10 cycles scanned at 30 mV s^{-1}. As can be seen, the highest value of current and capacity was obtained for the AEGO Nsh electrode prepared in K_2SO_4 solution.

In order to compare the electrochemical performance of the synthesized electrodes, their specific capacity (Csp) and electrochemical active surface areas (ECSAs) were calculated according to Eqs. 7 and 8:[57–59].

$$C_{sp} = \frac{1}{2\Delta V sv} \int_{V1}^{V2} i\,(V)\,dV \tag{7}$$

$$ECSAs = Cdl/Csp \tag{8}$$

In Eq. 7, S (cm^2) is the surface area of the substance, υ is the scan rate (V s^{-1}), ΔV is the potential window of CV, and i (A) represents the response current. The calculations of Csp for anodized electrodes in different

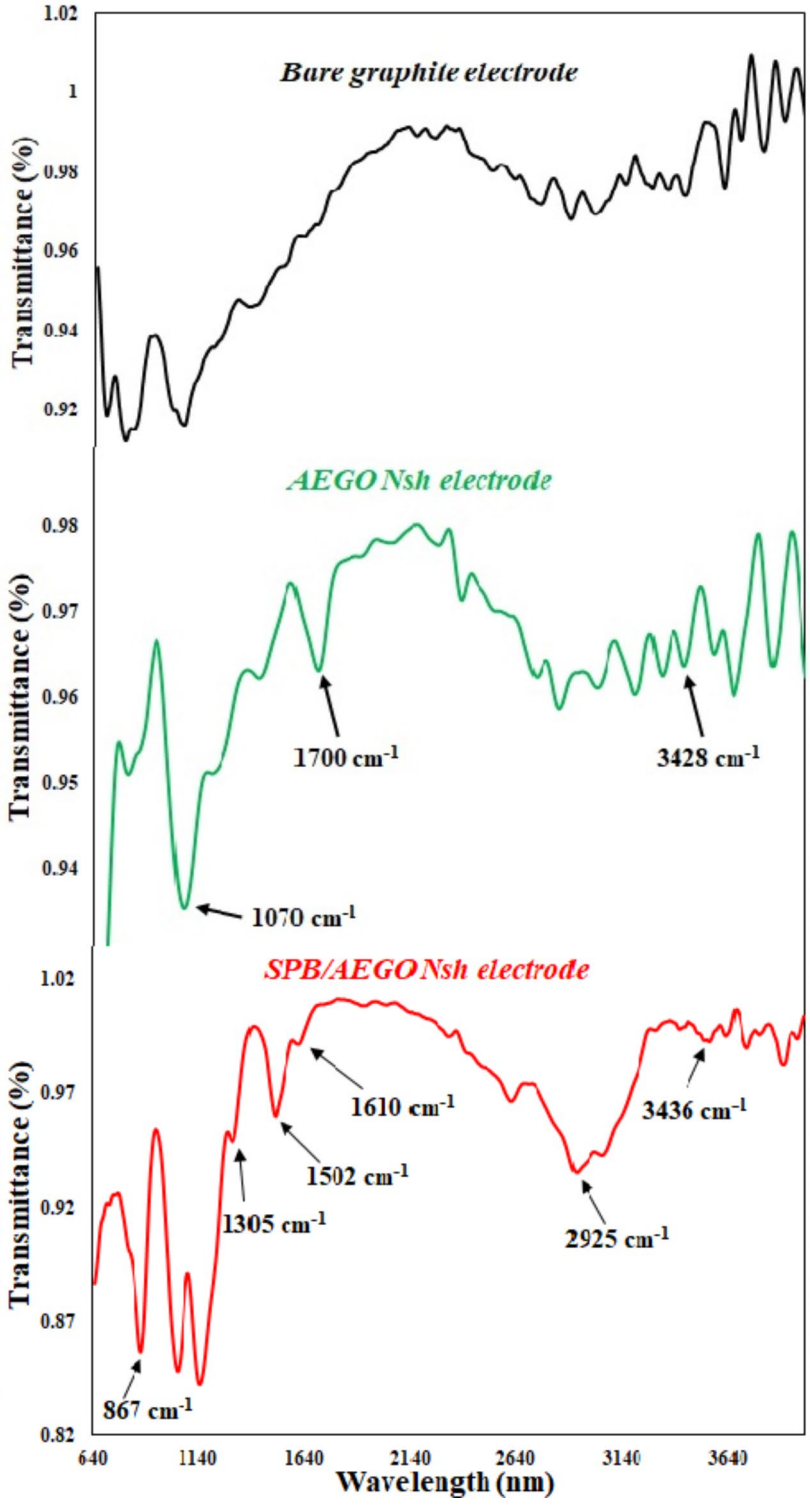

Fig. 7. ATR-IR spectra of the different electrode.

electrolyte solutions showed that the anodized electrode in the K_2SO_4 solution and then the Self-polymerization of benzidine on it has a higher specific capacity (335.40 mF/cm^2) than the anodized electrodes in $NaHCO_3$ (123.15 mF/cm^2) and H_2SO_4 (241.40 mF/cm^2) solutions. It's possible that the cause of this process can be related to the better performance of K_2SO_4 electrolyte solution in the anodizing process. In Eq. 8, C_{dl} is the double layer capacitance that was determined from a CV using the equation: $C_{dl} = \Delta j\ (ja\text{-}jc)/2\ \upsilon$, where ja and jc are anodic and cathodic current densities at $\Delta E = 0.5$ V, υ is the scan rate (mV/s) and Csp is the specific capacitance. The

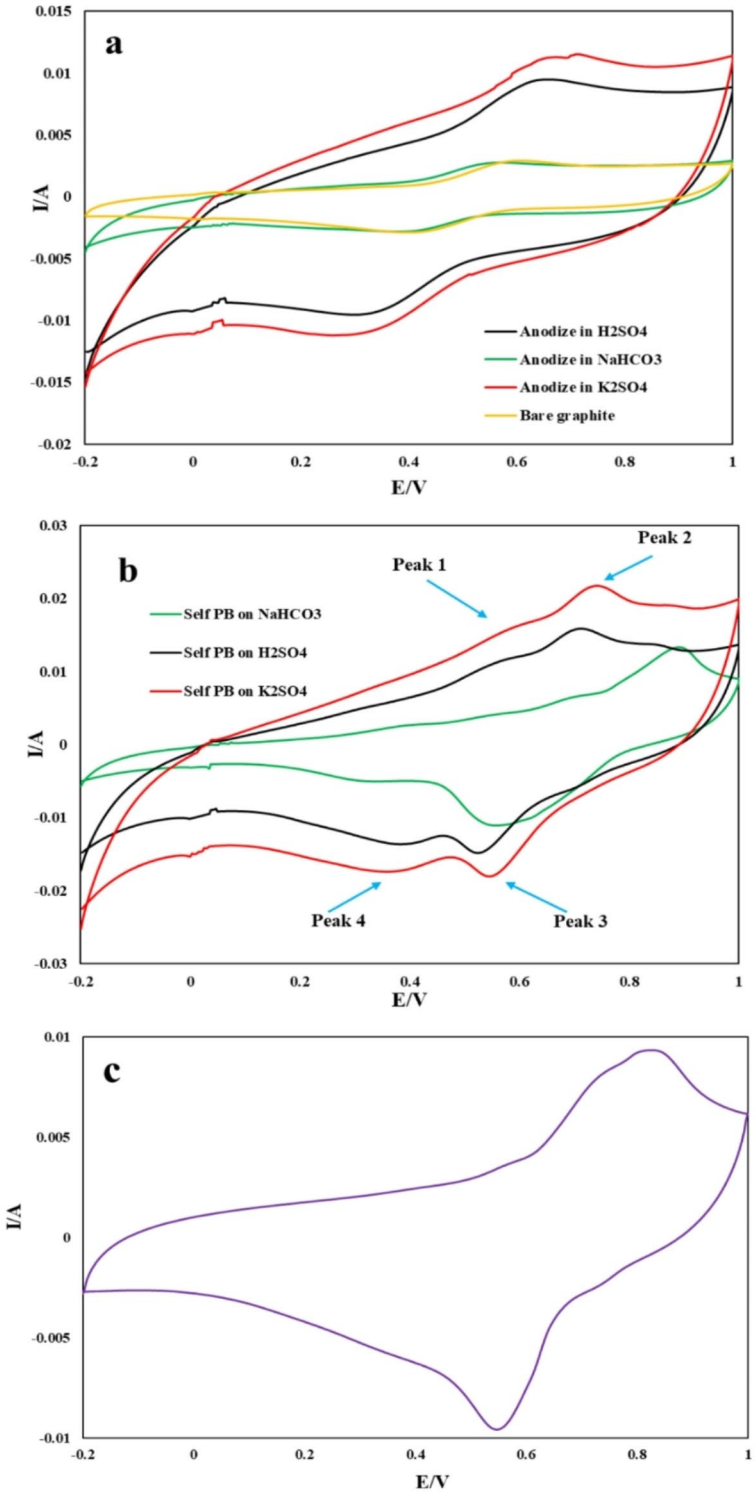

Fig. 8. CV plot of bare graphite electrode and AEGO Nsh electrodes that are anodized in different solutions (**a**), self-polymerization of PB in CH_3COOH on AEGO Nsh electrodes that are anodized in different solutions (**b**), and CV plot for the PB that is electropolymerized onto a graphite sheet in 1 M H_2SO_4 (**c**).

calculations of ECSAs for all three electrodes anodized in $NaHCO_3$ (1.63 cm^2), H_2SO_4 (1.60 cm^2), and K_2SO_4 (1.43 cm^2) solutions show that their ECSAs are not meaningfully different from each other.

In general, in this work, the purpose of this test was to observe the redox peaks of the benzidine polymer, which, as it is clear in the relevant curves, the redox peaks of the PB have fully appeared. For further proof, according to previous studies[33], PB was electrochemically polymerized on a bare graphite sheet and then its

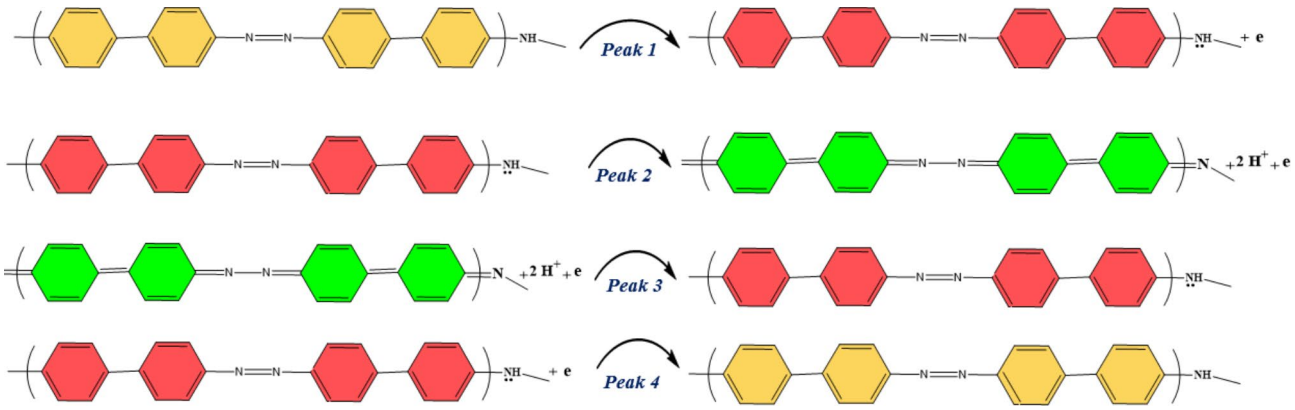

Fig. 9. The redox reaction mechanism of PB in 1.0 M H_2SO_4 solution.

behavior was investigated by CV (Fig. 8c). As shown in Fig. 8c, the peaks that appeared for PB correspond to the redox peaks that appeared for SPB, which once again confirmed the successful self-polymerization process.

According to curve 8b, it is clear that four redox peaks have appeared for PB, which can be related to the electron transfer process in the polymer structure. The redox reaction mechanisms of PB peaks are reported in Fig. 9. All the peaks observed for the SPB/AEGO Nsh electrode, where the benzidine monomer is self-polymerized on the AEGO Nsh electrode, are exactly according to the previous studies, in which various types of oxidizing agents and radical initiators were used for the polymerization process[28,60,61].

The EIS technique was studied to more evaluate the electrochemical processes occurring on different synthesis electrodes. This technique shows the effect of different frequencies on materials as well as the conductivity of the system[15]. Important information of this technique can be obtained from the Nyquist diagram. This graph consists of a small semi-circle section at high frequencies and a flat sloping line (Warburg line) at low frequencies[62]. Two important parameters obtained from the Nyquist plot include: (1) solution resistance (Rs, intersection point of Nyquist diagram with X-axis at high frequencies) and (2) charge transfer resistance (Rct, small diameter half ring)[15,32]. The EIS test of the electrodes was performed in 1M H_2SO_4 solution and the configuration of three electrodes in the frequency range of 100 Hz to 100 kHz in OCP potential. Figure 10a shows the Nyquist plot of bare graphite, AEGO Nsh, and SPB/AEGO Nsh electrodes. As it is clear in these plots, the R_s and R_{ct} for SPB/AEGO Nsh electrode are lower than that of bare graphite and AEGO Nsh electrodes, which indicates an increase in conductivity and the easy hydronium ions diffusion process on the SPB/AEGO Nsh electrode compared to the bare graphite and AEGO Nsh electrode[15,32]. Also, the steep slope of the Warburg line for the SPB/AEGO Nsh electrode compared to the bare graphite and AEGO Nsh electrodes shows the ideal capacitive behavior of this electrode after self-polymerization of benzidine. The results obtained from the EIS test showed that the increase in conductivity and the decrease in R_s and R_{ct} (R_p) as well as the formation of the ideal capacitor behavior of the SPB/AEGO Nsh electrode are due to the formation of benzidine polymer chains on the AEGO Nsh electrode. Also, the fitted Nyquist plot with the equivalent circuit related to SPB/AEGO Nsh electrode in OCP potential is depicted in Fig. 10b. Finally, the electrochemical tests of CV and EIS also confirmed the claim of the self-polymerization process.

Conclusions

We demonstrated that the self-polymerization of benzidine as a green, fast, cheap, simple, and energy-free method can take place on anodized graphite sheet. The characteristic results of surface morphology (FE-SEM) and chemical characteristics (XPS and ATR-IR analysis) of the SPB/AEGO Nsh electrode confirmed the spontaneous formation of PB on the AEGO Nsh electrode. Also, an investigation of the electrochemical behavior of the SPB/AEGO Nsh electrode showed that the self-polymerization of benzidine has been done successfully on the AEGO Nsh electrode. The present study showed that the self-polymerization of benzidine on the AEGO Nsh electrode is due to the presence of hydroxyl radicals and trapped electrons between GO nanosheets and graphite layers during the anodizing process. Finally, we believe that the use of this method and substrate is a starting point as a simple, cheap, and strong way for polymerization and identification of other aromatic diamine compounds and application in various industries.

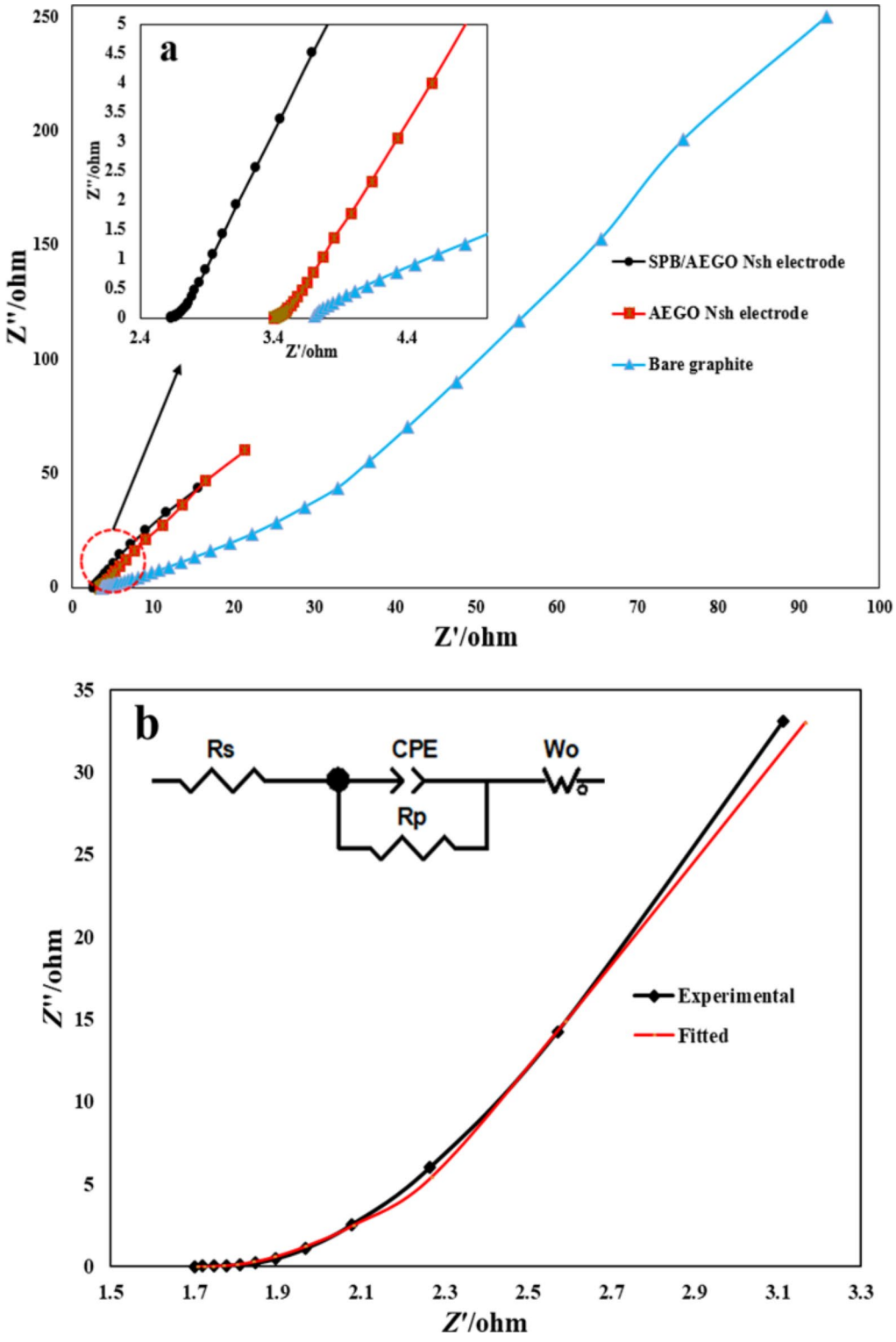

Fig. 10. Nyquist plot of different electrode and fitted Nyquist plot of SPB/AEGO Nsh electrode with the equivalent circuit related (b) in OCP potential and 1.0 M H_2SO_4 electrolyte solution.

Data availability

"The datasets used and/or analyzed during the current study are available from the corresponding author on reasonable request".

Received: 28 August 2024; Accepted: 6 November 2024
Published online: 12 November 2024

References

1. AlMaadeed, M. A. A., Ponnamma, D. & El-Samak, A. A. Elsevier,. Polymers to improve the world and lifestyle: Physical, mechanical, and chemical needs. In *Polymer science and innovative applications* 1–19 (2020).
2. Poddar, A. K., Patel, S. S. & Patel, H. D. Synthesis, characterization and applications of conductive polymers: A brief review. *Polym. Adv. Technol.* **32**, 4616–4641 (2021).
3. Awuzie, C. I. Conducting polymers. *Mater. Today Proc.* **4**, 5721–5726 (2017).
4. Garra, P. et al. Redox two-component initiated free radical and cationic polymerizations: Concepts, reactions and applications. *Prog Polym. Sci.* **94**, 33–56 (2019).
5. Hawker, C. J. Living free radical polymerization: A unique technique for the preparation of controlled macromolecular architectures. *Acc. Chem. Res.* **30**, 373–382 (1997).
6. Tadmor, Z. & Gogos, C. G. *Principles of Polymer Processing* (Wiley, 2013).
7. Gan, H. et al. Fabrication of polydiacetylene nanowires by associated self-polymerization and self-assembly processes for efficient field emission properties. *J. Am. Chem. Soc.* **127**, 12452–12453 (2005).
8. Lan, T., Kaviratna, P. D. & Pinnavaia, T. J. Epoxy self-polymerization in smectite clays. *J. Phys. Chem. Solids*. **57**, 1005–1010 (1996).
9. Ma, F. et al. Blend-electrospun poly (vinylidene fluoride)/polydopamine membranes: Self-polymerization of dopamine and the excellent adsorption/separation abilities. *J. Mater. Chem. A*. **5**, 14430–14443 (2017).
10. Thakur, V. K., Thakur, M. K., Raghavan, P. & Kessler, M. R. Progress in green polymer composites from lignin for multifunctional applications: A review. *ACS Sustain. Chem. Eng.* **2**, 1072–1092 (2014).
11. Postma, A. et al. Self-polymerization of dopamine as a versatile and robust technique to prepare polymer capsules. *Chem. Mater.* **21**, 3042–3044 (2009).
12. Liu, M. et al. Self-polymerization of dopamine and polyethyleneimine: Novel fluorescent organic nanoprobes for biological imaging applications. *J. Mater. Chem. B*. **3**, 3476–3482 (2015).
13. Chen, P. et al. A new self-polymerization of Acrylic Acid with a Mono-Aziridine containing compound. *J. Chin. Chem. Soc.* **57**, 901–908 (2010).
14. Dadashi, R., Bahram, M. & Faraji, M. Fabrication of symmetric solid-state Ni (OH) 2/MWCNT/ACG supercapacitor and more investigation of surface morphology on its capacitive behavior. *J. Mater. Sci. Mater. Electron.* **35**, 1–18 (2024).
15. Dadashi, R., Bahram, M. & Faraji, M. Fabrication of a solid-state symmetrical supercapacitor based on polyaniline grafted multiwalled carbon nanotube deposit onto created vertically oriented Graphene nanosheets on graphite sheet. *J. Energy Storage*. **52**, 104775 (2022).
16. Alanyalıoğlu, M., Segura, J. J. & Oro-Sole, J. Casan-Pastor, N. The synthesis of graphene sheets with controlled thickness and order using surfactant-assisted electrochemical processes. *Carbon N Y*. **50**, 142–152 (2012).
17. Munuera, J. M., Paredes, J. I., Villar-Rodil, S., Martínez-Alonso, A. & Tascón, J. M. D. A simple strategy to improve the yield of graphene nanosheets in the anodic exfoliation of graphite foil. *Carbon N Y*. **115**, 625–628 (2017).
18. Lee, H., Choi, J., Il, Park, J., Jang, S. S. & Lee, S. W. Role of anions on electrochemical exfoliation of graphite into graphene in aqueous acids. *Carbon N Y*. **167**, 816–825 (2020).
19. Ismail, H. K., Omer, R. A., Azeez, Y. H., Omar, K. A. & Alesary, H. F. Synthesis, characterization, and computational insights into the Conductive poly (p-aminophenol). *Russ J. Phys. Chem. B*. **18**, 1148–1165 (2024).
20. Momin, Z. H., Ahmed, A. T. A., Malkhede, D. D. & Koduru, J. R. Synthesis of thin-film composite of MWCNTs-polythiophene-Ru/Pd at liquid-liquid interface for supercapacitor application. *Inorg. Chem. Commun.* **149**, 110434 (2023).
21. Wang, C. et al. MnO2@ polypyrrole composite with hollow microsphere structure for electrode material of supercapacitors. *J. Electroanal. Chem.* **901**, 115780 (2021).
22. Shaheen Shah, S. et al. Recent progress in Polyaniline and its composites for supercapacitors. *Chem. Rec* e202300105 (2023).
23. Abd Ali, L. I. et al. Polypyrrole-coated zinc/nickel oxide nanocomposites as adsorbents for enhanced removal of pb (II) in aqueous solution and wastewater: An isothermal, kinetic, and thermodynamic study. *J. Water Process. Eng.* **64**, 105589 (2024).
24. Ali, L. I. A., Ismail, H. K., Alesary, H. F. & Aboul-Enein, H. Y. A nanocomposite based on polyaniline, nickel and manganese oxides for dye removal from aqueous solutions. *Int. J. Environ. Sci. Technol.* **18**, 2031–2050 (2021).
25. Qader, I. B. et al. Electrochemical sensor based on polypyrrole/triiron tetraoxide (PPY/Fe3O4) nanocomposite deposited from a deep eutectic solvent for voltammetric determination of procaine hydrochloride in pharmaceutical formulations. *J. Electroanal. Chem.* **951**, 117943 (2023).
26. Mohammed, M. Q., Ismail, H. K., Alesary, H. F. & Barton, S. Use of a Schiff base-modified conducting polymer electrode for electrochemical assay of cd (II) and pb (II) ions by square wave voltammetry. *Chem. Pap*. **76**, 715–729 (2022).
27. Ismail, H. K., Qader, I. B., Alesary, H. F., Kareem, J. H. & Ballantyne, A. D. Effect of graphene oxide and temperature on electrochemical polymerization of pyrrole and its stability performance in a novel eutectic solvent (choline chloride–phenol) for supercapacitor applications. *ACS Omega*. **7**, 34326–34340 (2022).
28. Dadashi, R., Bahram, M. & Farhadi, K. In-situ growth of Cu nanoparticles-polybenzidine over GO sheets onto graphite sheet as a novel electrode material for fabrication of supercapacitor device. *J. Energy Storage*. **79**, 110038 (2024).
29. Ekincī, E., Özden, M., Türkdemīr, M. H. & Karagözler, E. Preparation and properties of polybenzidine film-coated electrode as an H_2O_2 selective polymeric material. *J. Appl. Polym. Sci.* **70**, 2227–2234 (1988).
30. D'Eramo, F., Silber, J. J., Arévalo, A. H. & Sereno, L. E. Electrochemical detection of silver ions and the study of metal–polymer interactions on a polybenzidine film electrode. *J. Electroanal. Chem.* **494**, 60–68 (2000).
31. Shahsavani, A., Aladaghlo, Z. & Fakhari, A. R. Dispersive magnetic solid phase extraction of triazole fungicides based on polybenzidine/magnetic nanoparticles in environmental samples. *Microchim Acta*. **190**, 377 (2023).
32. Dadashi, R., Bahram, M. & Faraji, M. Polyaniline-tungsten oxide nanocomposite co-electrodeposited onto anodized graphene oxide nanosheets/graphite electrode for high performance supercapacitor device. *J. Appl. Electrochem.* **53**, 893–908 (2023).
33. Prasad, B. B., Srivastava, A., Pandey, I. & Tiwari, M. P. Electrochemically grown imprinted polybenzidine nanofilm on multiwalled carbon nanotubes anchored pencil graphite fibers for enantioselective micro-solid phase extraction coupled with ultratrace sensing of d-and l-methionine. *J. Chromatogr. B*. **912**, 65–74 (2013).
34. Cai, W. et al. Synthesis and solid-state NMR structural characterization of 13 C-labeled graphite oxide. *Sci. (80-)*. **321**, 1815–1817 (2008).
35. Boukhvalov, D. W. & Katsnelson, M. I. Modeling of graphite oxide. *J. Am. Chem. Soc.* **130**, 10697–10701 (2008).
36. Lee, N. E., Lee, J., Jeong, H. Y., Lee, S. Y. & Cho, S. O. Vertically aligned graphene prepared by the electrochemical anodization of graphite foil for supercapacitor electrodes. *J. Power Sources*. **526**, 231137 (2022).
37. Zhang, G., Wen, M., Wang, S., Chen, J. & Wang, J. Insights into electrochemical behavior and anodic oxidation processing of graphite matrix in aqueous solutions of sodium nitrate. *J. Appl. Electrochem.* **46**, 1163–1176 (2016).
38. Goss, C. A., Brumfield, J. C., Irene, E. A. & Murray, R. W. Imaging the incipient electrochemical oxidation of highly oriented pyrolytic graphite. *Anal. Chem.* **65**, 1378–1389 (1993).
39. Hathcock, K. W., Brumfield, J. C., Goss, C. A., Irene, E. A. & Murray, R. W. Incipient electrochemical oxidation of highly oriented pyrolytic graphite: Correlation between surface blistering and electrolyte anion intercalation. *Anal. Chem.* **67**, 2201–2206 (1995).
40. Li, M., Yin, W., Han, X. & Chang, X. Hierarchical nanocomposites of polyaniline scales coated on graphene oxide sheets for enhanced supercapacitors. *J. Solid State Electrochem.* **20**, 1941–1948 (2016).
41. Shao, D. et al. PANI/GO as a super adsorbent for the selective adsorption of uranium (VI). *Chem. Eng. J.* **255**, 604–612 (2014).

42. Wang, X. et al. Interface polymerization synthesis of conductive polymer/graphite oxide@ sulfur composites for high-rate lithium-sulfur batteries. *Electrochim. Acta*. **155**, 54–60 (2015).
43. Peng, H. et al. A novel fabrication of nitrogen-containing carbon nanospheres with high rate capability as electrode materials for supercapacitors. *Rsc Adv.* **5**, 12034–12042 (2015).
44. Xu, B., Zheng, D., Jia, M., Cao, G. & Yang, Y. Nitrogen-doped porous carbon simply prepared by pyrolyzing a nitrogen-containing organic salt for supercapacitors. *Electrochim. Acta*. **98**, 176–182 (2013).
45. Golczak, S., Kanciurzewska, A., Fahlman, M., Langer, K. & Langer, J. J. Comparative XPS surface study of polyaniline thin films. *Solid State Ionics*. **179**, 2234–2239 (2008).
46. Deng, J., Wang, T., Guo, J. & Liu, P. Electrochemical capacity fading of polyaniline electrode in supercapacitor: An XPS analysis. *Prog Nat. Sci. Mater. Int.* **27**, 257–260 (2017).
47. Chen, W. C., Wen, T. C. & Gopalan, A. Negative capacitance for polyaniline: An analysis via electrochemical impedance spectroscopy. *Synth. Met.* **128**, 179–189 (2002).
48. Parvez, K. et al. Electrochemically exfoliated graphene as solution-processable, highly conductive electrodes for organic electronics. *ACS Nano*. **7**, 3598–3606 (2013).
49. Luckas, N. et al. Adsorption and reaction of SO2 on clean and oxygen precovered pd (100)—a combined HR-XPS and DF study. *Phys. Chem. Chem. Phys.* **13**, 16227–16235 (2011).
50. Kumar, N., Das, S., Bernhard, C., Varma, G. & Das Effect of graphene oxide doping on superconducting properties of bulk MgB2. *Supercond Sci. Technol.* **26**, 95008 (2013).
51. Anothumakkool, B., Bhange, S. N., Badiger, M. V. & Kurungot, S. Electrodeposited polyethylenedioxythiophene with infiltrated gel electrolyte interface: A close contest of an all-solid-state supercapacitor with its liquid-state counterpart. *Nanoscale*. **6**, 5944–5952 (2014).
52. Manivel, A., Sivakumar, R., Anandan, S. & Ashokkumar, M. Ultrasound-assisted synthesis of hybrid phosphomolybdate–polybenzidine containing silver nanoparticles for electrocatalytic detection of chlorate, bromate and iodate ions in aqueous solutions. *Electrocatalysis*. **3**, 22–29 (2012).
53. Mahore, P., Burghate, R. K., Kondawar, D. B. & Mahajan, S. P. V Nandanwar, D. Polypyrrole/MnO2 nanocomposites as potential electrodes for supercapacitor. *Adv. Mater. Lett.* **9**, 538–543 (2018).
54. Heinze, J. Cyclic voltammetry—electrochemical spectroscopy. New analytical methods (25). *Angew Chemie Int. Ed. Engl.* **23**, 831–847 (1984).
55. Parvez, K. et al. Exfoliation of graphite into graphene in aqueous solutions of inorganic salts. *J. Am. Chem. Soc.* **136**, 6083–6091 (2014).
56. Ossonon, B. D. & Bélanger, D. Functionalization of graphene sheets by the diazonium chemistry during electrochemical exfoliation of graphite. *Carbon N Y*. **111**, 83–93 (2017).
57. Dadashi, R., Faraji, M., Mostafazadeh, N. & Bahram, M. Fabrication of solid-state symmetrical supercapacitor device based on constructed novel Gr-Cu-MoO2 disk electrodes based on co-replacement reactions. *J. Power Sources*. **618**, 235206 (2024).
58. Schalenbach, M. et al. How microstructures, oxide layers, and charge transfer reactions influence double layer capacitances. Part 1: Impedance spectroscopy and cyclic voltammetry to estimate electrochemically active surface areas (ECSAs). *Phys. Chem. Chem. Phys.* **26**, 14288–14304 (2024).
59. Shrestha, N. K. et al. Chemical etching induced microporous nickel backbones decorated with metallic Fe@ hydroxide nanocatalysts: An efficient and sustainable OER anode toward industrial alkaline water-splitting. *J. Mater. Chem. A*. **10**, 8989–9000 (2022).
60. Dadashi, R., Farhadi, K. & Bahram, M. Polybenzidine-MnO2 nanocomposite on anodized graphite sheet as a novel system for high-performance supercapacitors. *Diam. Relat. Mater.* **110923** (2024).
61. Dadashi, R., Farhadi, K. & Bahram, M. Towards using polybenzidine-graphene oxide sheet on Graphite as a New System for Supercapacitor device fabrication. *J. Electrochem. Soc.* **171**, 060532 (2024).
62. Sunil, V., Pal, B., Misnon, I. I. & Jose, R. Characterization of supercapacitive charge storage device using electrochemical impedance spectroscopy. *Mater. Today Proc.* **46**, 1588–1594 (2021).

Acknowledgements

This work was partially supported by the Research Affairs of Urmia University.

Author contributions

R.Dadashi presented the main idea, performed the experiments and wrote the draft version of the manuscript. K.Farhadi contributed to the main idea and edited the manuscript. M.Bahram contributed to the main idea and edited the manuscript.

Declarations

Competing interests

The authors declare no competing interests.

Additional information

Correspondence and requests for materials should be addressed to K.F.

Reprints and permissions information is available at www.nature.com/reprints.

Publisher's note Springer Nature remains neutral with regard to jurisdictional claims in published maps and institutional affiliations.